Journal of Orthopaedic Translation 24 (2020) 198–208

Contents lists available at ScienceDirect

Journal of Orthopaedic Translation

journal homepage: www.journals.elsevier.com/journal-of-orthopaedic-translation

Original Article

# Promoting osteoblasts responses *in vitro* and improving osteointegration *in vivo* through bioactive coating of nanosilicon nitride on polyetheretherketone

Yong Dai [a,☆], Han Guo [b,e,**], Linyang Chu [c,☆], Zihao He [c], Minqi Wang [c], Shuhong Zhang [c], Xifu Shang [d,*]

[a] *Shandong University, Jinan, 250012, Shandong, China*
[b] *Shanghai Institute of Applied Physics, CAS, 2019 Jialuo Road, Shanghai, 201800, China*
[c] *Shanghai Key Laboratory of Orthopaedic Implants, Department of Orthopaedic Surgery, Shanghai Ninth People's Hospital, Shanghai Jiao Tong University School of Medicine, Shanghai, 200011, China*
[d] *Department of Orthopaedic Surgery, The First Affiliated Hospital of USTC, Division of Life Sciences and Medicine, University of Science and Technology of China, Hefei, 230001, Anhui, China*
[e] *Shanghai Synchrotron Radiation Facility, Shanghai Advanced Research Institute, CAS, 239 Zhangheng Road, Shanghai, 201204, China*

ARTICLE INFO

*Keywords:*
Cells responses
Coating
Osseointegration
Polyetheretherketone
Silicon nitride

ABSTRACT

*Objective:* To enhance the bioactivity of polyetheretherketone (PEEK) while maintain its mechanical strengths.
*Methods:* Suspension coating and melt bonding.
*Results:* Silicon nitride ($Si_3N_4$, SN) coating lead to higher surface roughness, hydrophilicity and protein absorption; SN coating could slowly release Si ion into simulated body fluid (SBF), which caused weak alkaline of micro-environment owing to the slight dissolution of SN; SN coating resulted in the improvements of adhesion, proliferation, differentiation and gene expressions of MC3T3-E1 cells *in vitro*; SN coating of PEEK with bioactive SN coating (CSNPK) obviously promoted bone regeneration and osseointegration *in vivo*.
*Conclusions:* CSNPK with SN coating as bone implant might be a promising candidate for orthopedic implants.
*The Translational Potential of this Article:* The silicon nitride-coated polyetheretherketone (CSNPK) prepared in this article could induce MC3T3-E1 cells adhesion, proliferation and differentiation *in vitro*; it could also induce bone regeneration in bone defect *in vivo*, which indicate its good cytocompatibility and biocompatibility. If the raw materials are medical grade, and preparation process as well as production process of this article are further improved, it will have great translational potential.

## Introduction

Polyetheretherketone (PEEK), a special function thermoplastic, has been widely applied as bone implants for orthopaedic and dental applications [1]. PEEK has garnered considerable attention due to many advantages, including excellent biocompatibility and chemical resistance, high mechanical properties, and elasticity modulus closer to that of natural bone [1–3]. With the expanded applications of PEEK as permanent orthopaedic and spinal implants, attention raised concerning its osseointegration that has significant effects on the initial load/fixation and long-term stability of implants [4]. However, PEEK is not a bioactive material, which exhibits poor osseointegration due to its bioinert nature [5]. Therefore, how to improve the bioactivity of PEEK has been one of the challenges in orthopaedic applications.

Many efforts have been devoted to developing novel modifications of PEEK to improve bioactivity and accelerate osseointegration. These efforts included physical blending PEEK with bioactive materials (e.g., hydroxyapatite, titanium dioxide, calcium silicate, and so on), surface treatment (e.g., plasma treatment), surface functionalisation (e.g., grafting functional groups), and surface coating (e.g., biomolecule, bioactive materials) [3,6–8]. Blending bioactive materials into PEEK mitrix to fabricate PEEK-based composites increased the bioactivity of

* Corresponding author. Department of Orthopaedic Surgery, The First Affiliated Hospital of USTC, Division of Life Sciences and Medicine, University of Science and Technology of China, Hefei, 230001, Anhui, China.
** Corresponding author. Shanghai Institute of Applied Physics, CAS, 2019 Jialuo Road, Shanghai 201800, China.
*E-mail addresses:* guohan@sinap.ac.cn (H. Guo), shangxifuchina@163.com (X. Shang).
☆ These authors contributed equally to this study.

https://doi.org/10.1016/j.jot.2019.10.011
Received 17 July 2019; Received in revised form 20 October 2019; Accepted 28 October 2019
Available online 21 November 2019

PEEK but decreased the mechanical strength [9]. The strategy of physical/chemical treatment (e.g., plasma treatment, grafting specific functional groups and coating of biomolecules) improved biological properties of PEEK; however, these surface modifications might not be practical in clinic applications due to their unstable properties [10]. Hence, it is an important requirement for development of new technology of surface modification for improving the bioactivity of PEEK.

As a nonoxide ceramic, silicon nitride ($Si_3N_4$, SN) has been used in industry known for its high performances (e.g., high mechanical strength, thermal stability, and excellent corrosion resistance) [11,12]. In the past few years, SN ceramic has been investigated as biomedical material and medical device for bone implant because of excellent biocompatibility and bioactivity [13,14]. Spinal fusion devices and intervertebral discs made of SN ceramics have been used in clinic for many years [15]. Silicon and nitrogen were deposited into the crystal lattice of native hydroxyapatite by action of the osteoblasts, which was confirmed by chemical and spectroscopy analyses of the SN spinal implant [16]. Silicon and nitrogen were key components for the upregulation of osseous activity, which ultimately resulted in accelerated bone regeneration [16,17]. SN is very biocompatible and bioactive, which showed excellent bone affinity [18]. Therefore, SN ceramic has attracted more attention as a promising candidate for use as a skeletal prosthetic implant.

In this work, to enhance the bioactivity of PEEK while maintaining its mechanical strengths, bioactive SN was coating of silicon nitride on PEEK (CSNPK) by a method of suspension coating and melt bonding. The aim of this study is to prepare a bioactive SN coating with micro/nano structures on PEEK (CSNPK) surface, which could induce osteoblasts positive responses *in vitro*, and promote bone regeneration as well as osseointegration *in vivo*. Therefore, the effects of SN coating on the surface properties (morphology, micro/nano structure, roughness, hydrophilicity, protein absorption, and Si ion release) of CSNPK and on the responses of MC3T3-E1 cells *in vitro* were studied. Moreover, the effects of SN coating on bone regeneration and osseointegration of CSNPK *in vivo* by using the defects of skull model of rats were evaluated.

## Materials and methods

### *Preparation and characterisation of samples*

Nano $Si_3N_4$ (β phase, 99.9% metals basis, Aladdin Industrial Co., Ltd., China) coating on PEEK (CSNPK) was prepared through a method of suspension coating and melt bonding. Briefly, 30 g PEEK (OXPK-C, Oxford Performance Materials, UK) powders were dispersed into 600 mL ethanol solution and stirred with ultrasonic for 2 h. Then the dispersion was centrifuged and dried at 40 °C in an oven (DHG-9070A, Bluepard, Shanghai, China). By using the obtained powders, the samples with the sizes of Φ12 × 2 mm (for material characterisation and *in vitro* cell experiments) and Φ4 × 5 mm (*in vivo* animal experiments) were prepared through cold pressing method. The as-prepared samples were sintered at 345 °C for 6 h in a muffle furnace (SX2-2.5-10NP, Yiheng, Shanghai, China). Then, the samples were polished by 1500 grit abrasive papers and cleaned ultrasonically in ethanol and deionized water sequentially. After that, the samples were air-dried at 40 °C for overnight to acquire dense sample of PEEK. The samples of PEEK were soaked into ethanol suspension with nano-SN (20 wt%) and stirred continuously for 24 h. Afterwards, the samples of PEEK with SN coating were resintered at 345 °C for 6 h to obtain CSNPK. The PEEK samples without SN coating were defined as controls. The scanning electron microscope (SEM; S-4800, Hitachi Co., Tokyo, Japan) and energy dispersive spectroscopy (EDS, Hitachi Co., Tokyo, Japan) were used to determine PEEK and CSNPK surface morphology and elemental composition.

### *Adhesive strength, surface roughness, and hydrophilicity of coating*

Adhesive strength of the SN coating with PEEK substrate was determined by using universal testing machine (E45.305, China). In brief, the coated side of the sample was attached to the clamping fixture (70 mm × 50 mm × 50 mm) using E-7 glue, and the load force was continuously applied at a loading speed of 3 mm/min until the sample was broken. The adhesive strength F of the SN coatings was calculated by the following formula: F = fmax/A, where fmax is the measured peak of load force and A is the area of the SN film. The laser confocal 3D microscope (VK-X 110, Keyence Co., Japan) was used to determine the surface morphology and roughness of the samples. The hydrophilicity of the samples was determined by testing the water contact angles using a contact angle-measuring device (JC2000D2, Shanghai zhongchen digital technic apparatus Co., Ltd., China).

### *Adsorption of protein, changes of ions concentrations, and pH values in simulated body fluid*

Bovine serum albumin (BSA) and fibronectin (Fn) were used to determine the protein adsorption of the samples. Each sample in a 24-well plate was added of 1 mL of dulbecco's modified eagle medium (DMEM) (Gibco BRL, Thermo Fisher Scientific, USA) containing BSA (BioFroxx, Germany 10 μg/mL) and Fn (Sigma, Tokyo, Japan, 10 μg/mL), respectively. After incubation for 2 and 4 h, the unadsorbed proteins were washed away by phosphate-buffered saline solution, and the adsorbed proteins on the surfaces of PEEK and CSNPK were detached by 500 μL sodium dodecyl sulphate solution and measured by bicinchoninic acid protein assay.

The changes of Si ion concentration at each time point (1, 3, 5, 7, 10, 14, 21, and 28 days) were tested using inductively coupled plasma (ICP) (AES, Varian 710-ES, Agilent Technologies, USA) after the samples were immersed into simulated body fluid (SBF) solution at the cell culture conditions (37 °C, 5% $CO_2$ and humidified atmosphere of 95% air). At each time point (6, 12, 24, 72, 120, and 168 h), the pH values were tested by a flat membrane microelectrode (PB-10, Germany). After soaked for 28 days, the adhesive strength of the SN coating of CSNPK was measured by universal testing machine (E45.305, China) at a loading speed of 3 mm/min.

### *Cytocompatibility in vitro*

#### *Cell attachment and proliferation*

Mouse osteoblast-like MC3T3-E1 cells were used to evaluate the cytocompatibility of the samples *in vitro*. The samples of PEEK and CSNPK were sterilised by ethylene oxide and placed in 24-well plates. The cells suspension was cultured on the samples at a density of $2 \times 10^4$/$cm^2$ per well with the addition of Dulbecco's Modified Eagle Medium (DMEM; Thermo Fisher Scientific Inc., USA) containing 10% foetal bovine serum (Hyclone, Tauranga, New Zealand) and streptomycin 100 ug/mL and antibiotics (penicillin 100U/mL).

The cell counting kit-8 (CCK-8) was performed to assess cell adhesion on the samples at 6 and 12 h and cell proliferation on the samples at 1, 4, and 7 days. The optical density (OD) values of experimental group ($OD_E$), control group ($OD_C$), and blank group ($OD_B$) were measured at 6 and 12 h, and the cell attachment ratio was calculated by using following formula: cell attachment ratio = ($OD_E$-$OD_B$)/($OD_C$-$OD_B$) × 100%. Moreover, to calculate the proliferation rate of cells, the modified OD values at 4 and 7 days were normalised to those at 1 day [19]. For different time, the samples were washed twice with sterile phosphate-buffered saline and replaced by 1 mL of the fresh medium with 10% CCK-8 solution (Dojindo Molecular Technologies Inc., Kumamoto, Japan). After culturing for 3 h, 100 μL of the medium was transferred to a 96-well plate for measurement. The OD values were measured by using a Synergy HT microplate reader (Bio-Tek Instruments Ltd, Winooski, VT, USA) at a wavelength of 450 nm.

Meanwhile, at 12 and 24 h after culturing, the cells on samples were fixed with 4% paraformaldehyde for 15 min. Then, the cells nuclei were stained with 4,6-diamino-2-phenylindole (DAPI, Molecular Probe,

Sigma–Aldrich) for 15 min and cells cytoskeleton were stained with rhodamine phalloidin (5 units·mL$^{-1}$; Biotium, Hayward, CA, USA) for 30 min, respectively. Then the confocal laser scanning microscopy (Nikon AIR, Nikon, Japan) was used to observe them.

*Cell morphology and spreading*

After cultured for 12 h, 2.5% glutaraldehyde was used to fix the cells on samples for 1 h. Then, the cells were dehydrated for 10 min with 10%, 30%, 50%, 70%, 80%, 90%, and 100% ethanol solution, respectively. After that, the samples were air-dried at 37 °C. SEM was used to observe the morphology of the cells on samples.

*Alkaline phosphatase staining and quantitative analysis of alkaline phosphatase activity*

The MC3T3-E1 cells were seeded on PEEK and CSNPK at a density of $2 \times 10^4/cm^2$. After culturing for 24 h, the medium was refreshed by osteogenic induction medium contained α-MEM, 10% foetal bovine serum (Hyclone, Tauranga, New Zealand), penicillin (100 μg/mL), 1% streptomycin (100 mg/mL), 100 nM dexamethasone (Sigma–Aldrich), and ascorbic acid (50 μg/mL). The cell osteogenic induction medium was refreshed every two days.

At 7, 14, and 21 days after culturing, alkaline phosphatase (ALP) staining was carried out by the previous published procedures [19]. The ALP activity was determined by ALP activity assay kit (P0321, Beyotime, China). For normalisation, the total protein content was determined by bicinchoninic acid protein assay kit (Thermo Fisher Science) in terms of the provided instructions.

*Alizarin-red staining and quantitative evaluation of mineralised nodules*

Alizarin-red staining (ARS) was performed to determine the formation of mineralised nodules of the cells on the samples. At 21 and 28 days after culturing, the cells on samples were fixed with 4% paraformaldehyde for 30 min and then stained with 1% alizarin red solution (Sigma) for 45 min. Then the samples were rinsed with deionized water to elute the nonstaining and investigated by optical microscopy. Then calcium nodules were rinsed with 10% cetylpyridinium chloride (Sigma–Aldrich) for quantitative analysis at wavelengths of 620 nm using the microplate reader.

*Bone-related genes expression*

The expression of bone-related genes, including ALP, osteopontin (OPN), collagen type I (COLI), and osteocalcin (OCN), were quantitatively tested by real-time polymerase chain reaction (PCR) with diaminopimelate dehydrogenase (DAPDH) as the housekeeping gene for normalisation. The forward and reverse primers for different genes are listed in Adhesive strength. At 7, 14, and 21 days after culturing, the total RNA from the cell lysates were extracted using Trizol reagent (Invitrogen, Carlsbad, CA, USA) in terms of the manufacturer's protocol. The reverse transcription was carried out by PrimeScript® real time (RT) reagent kit (Takara Bio-technology Co., Dalian, China). The quantitative PCR was carried out on an ABI 7500 machine (Applied Biosystems, USA) by SYBR premix EX Taq PCR kit (Takara). The primer sequences for real-time PCR were listed in Table 1.

*In vivo osteogenesis*

*Model of skull defects*

Twenty Sprague–Dawley (SD) rats aged 6 months were separated into 2 groups for the animal experiments, which were approved by the Institutional Ethics Committee of the Shanghai 9th People's Hospital, China. Briefly, the rats were anesthetised by intraperitoneal injection of chloral hydrate (1 mL/300 g). After the skull was sterilised by 2% iodine, the parietal calvarium bone defect with diameter of 4 mm was drilled with a trephine bur. After implanting the different samples (4 mm in diameter) in bone defects, and the incisions were sewed up layer by layer. At 4 and 8 weeks after operation, the rats were sacrificed and the skull bones were obtained, which were fixed in 10% neutral formalin buffer.

**Table 1**
Primer sequences for real-time PCR.

| Target gene | Primers (5′–3′; F = forward; R = reverse) | Length |
|---|---|---|
| ALP | F: GGGCATTGTGACTACCACTCG | 21 |
| | R: CCTCTGGTGGCATCTCGTTAT | 21 |
| COL1 | F: AACAGTCGCTTCACCTACAGC | 21 |
| | R: GGTCTTGGTGGTTTTGTATTCG | 22 |
| OPN | F: ATCTCACCATTCGGATGAGTCT | 22 |
| | R: TGTAGGGACGATTGGAGTGAAA | 22 |
| OCN | F: CTGACCTCACAGATCCCAAGC | 21 |
| | R: TGGTCTGATAGCTCGTCACAAG | 22 |
| GAPDH | F: AGGTCGGTGTGAACGGATTTG | 21 |
| | R: GGGGTCGTTGATGGCAACA | 19 |

ALP = alkaline phosphatase; COL1 = collagen type I; OCN = osteocalcin; OPN = osteopontin; PCR = polymerase chain reaction.

*Micro-computed tomography and histological analysis*

The samples were observed by micro–computed tomography (micro-CT). The newly formed bone (NB) within the bone defects was acquired for quantification of bone mineral density (BMD), tissue volume (TV), and bone volume (BV). Moreover, all samples were decalcified in a 17% ethylenediaminetetraacetic acid solution for 2 weeks using Rapid Decalcifier (DeCa DX-1000; Pro-Cure Medical Technology Co Ltd, Hong Kong). Then the samples were embedded in paraffin. Sections perpendicular to the long axis of the bone with the thickness of 5 μm were stained with hematoxylin/eosin (H&E) and Masson trichrome staining. These sections were digitalized into a microscopic system for descriptive histology of the appearance of the NB and quantitative histomorphometry.

*Statistical analysis*

The experiments were performed in triplicate and 3 duplicate samples in one group were used. The data were expressed as mean ± standard deviation. Statistical analysis was measured using one-way analysis of variance (ANOVA) and the least significant difference test followed by Mann–Whitney *U* test to determine the level of significance, using statistical product and service solutions (SPSS) software (v19.0, USA). The differences were considered statistically significant at $p$-value $< 0.05$ and significantly statistically significant at $p$-value $< 0.01$.

## Results

*Characteristics of SN coating of CSNPK*

Figure 1A and B shows the SEM images of PEEK surface morphology, which displayed smooth surface. Figure 1C–E reveals the SEM images of CSNPK surface morphology, which exhibited rough surface. In the high-magnification SEM images, the coating of CSNPK contained not only SN microparticles (Figure 1D) but also SN nanoparticles (Figure 1E). The SEM images of CSNPK cross-section is shown in Figure 1F. The SN coating thickness was approximately 10 μm, which was closely combined with the PEEK substrate. From the EDS of PEEK (Figure 1G) and CSNPK (Figure 1H), the peaks of carbon and oxygen elements appeared on PEEK surface while the peaks of carbon, oxygen, silicon, and nitrogen elements appeared on CSNPK.

*Roughness, hydrophilicity, and adhesive strength of SN coating on PEEK*

Figure 2A and B shows 3D images surface morphology of samples by laser microscope. PEEK displayed smooth surface while CSNPK with SN coating showed rough surface. The surface roughness (Ra) of PEEK and CSNPK was 3.992 μm and 8.290 μm, respectively ($p < 0.05$). In addition,

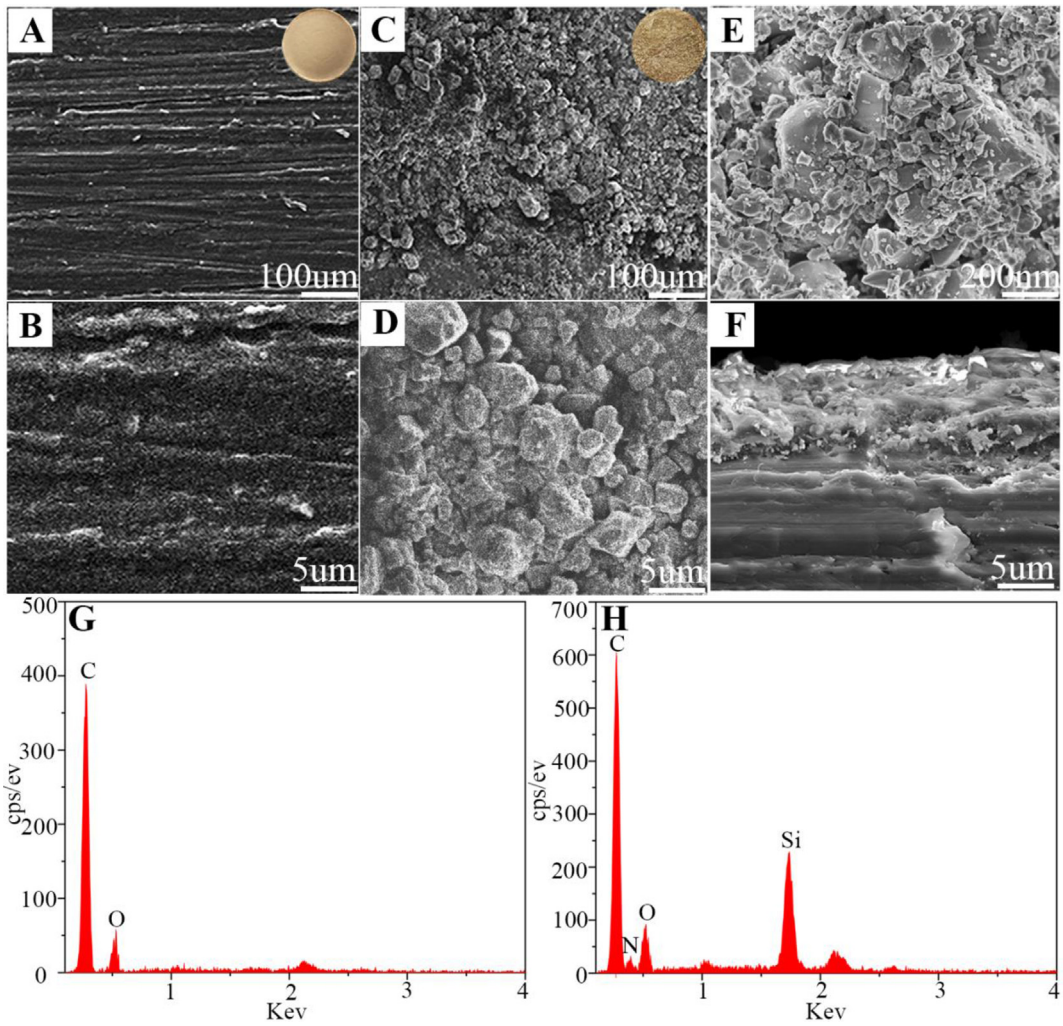


**Figure 1.** (A, B) SEM images of surface morphology of PEEK, (C, D, E) SEM images of surface morphology of CSNPK, (F) SEM images of cross-sectional of CSNPK, (G) EDS of PEEK, (H) EDS of CSNPK. EDS = energy-dispersive spectroscopy; PEEK = polyetheretherketone; SEM = scanning electron microscope.

the water contact angles of PEEK and CSNPK were 115.50° and 67°, respectively ($p < 0.05$). Moreover, the adhesive strength of the SN coating with the substrate of PEEK was 7.9 MPa ($p < 0.05$).

*Protein adsorption, Si ion release, and pH value change in SBF*

Figure 3A and B shows the adsorptions of both BSA and Fn on the samples. At 4 h, the adsorptions of BSA and FN for CSNPK were higher than PEEK ($p < 0.05$). After the samples soaking into SBF for different times, the variation of Si ion concentration is shown in Figure 3C. The Si ion concentration of CSNPK increased rapidly from the 1st to 14th day and stabilised from the 14th to 28th day. However, no Si ion release from PEEK into SBF was observed. Figure 3D shows the changes of pH values in solution after the samples soaking into SBF for each time point. No change of pH values with time for PEEK was found, whereas the pH values for CSNPK slightly increased with time. The pH value for CSNPK was around 7.6 at 168 h after soaking.

*In vitro evaluation of cells responses*

*Cell adhesion, morphology, and proliferation*

Figure 4 shows that the confocal laser scanning microscopy images of cells on the samples at 12 (Figure 4A) and 24 (Figure 4B) hours. At 12 h after culturing, the number of adhered cells on CSNPK was higher than PEEK. At both 12 and 24 h, compared with PEEK, the cells on CSNPK showed more lamellipodia and adhered more closely to the substrates ($p < 0.05$).

Figure 5 shows the SEM images of the cells on the samples at 12 h. The cells on PEEK (Figure 5A and B) surface exhibited spherical-like morphology without any spreading. However, the cells on CSNPK (Figure 5C and D) displayed spreading morphology with more pseudopods. Figure 5E shows that attachment ratio of the cells on CSNPK surface was higher than PEEK at 12 h ($p < 0.05$). Figure 5F shows that the OD values (proliferation) of the cells on CSNPK were higher than on PEEK at 4 and 7 days ($p < 0.05$).

*Osteogenic differentiation*

Figure 6A displays the ALP staining of cells on the samples at 7, 14, and 21 days after culturing. The intensity (staining) of ALP of cells on CSNPK was stronger than on PEEK, demonstrating that the differentiation of the cells on CSNPK was more than PEEK. Figure 6C exhibits the quantitative analysis of ALP activity of cells on the samples at 7, 14, and 21 days after culturing. The ALP activity of cells for CSNPK was higher than that for PEEK at 7, 14, and 21 days, demonstrating that the differentiation of the cells on CSNPK was more than that on PEEK.

Figure 6B shows the ARS staining of cells on the samples after culturing at 21 and 28 d. The intensity (staining) of ARS on CSNPK was stronger than on PEEK, indicating that the mineralised nodules on CSNPK were more than those on PEEK. Figure 6D shows the quantitative analysis

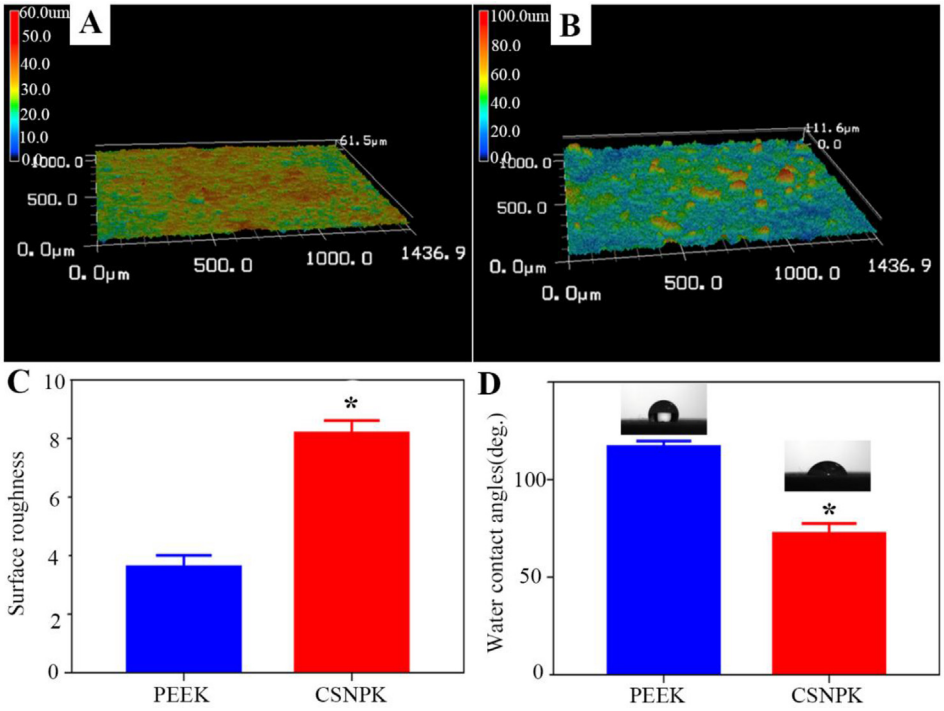


**Figure 2.** (A) Laser microscope 3D images of surface morphology of PEEK, (B) Laser microscope 3D images of surface morphology of CSNPK, (C) Surface roughness of PEEK, (D) Surface roughness of CSNPK (* represent $p < 0.05$). PEEK = polyetheretherketone.

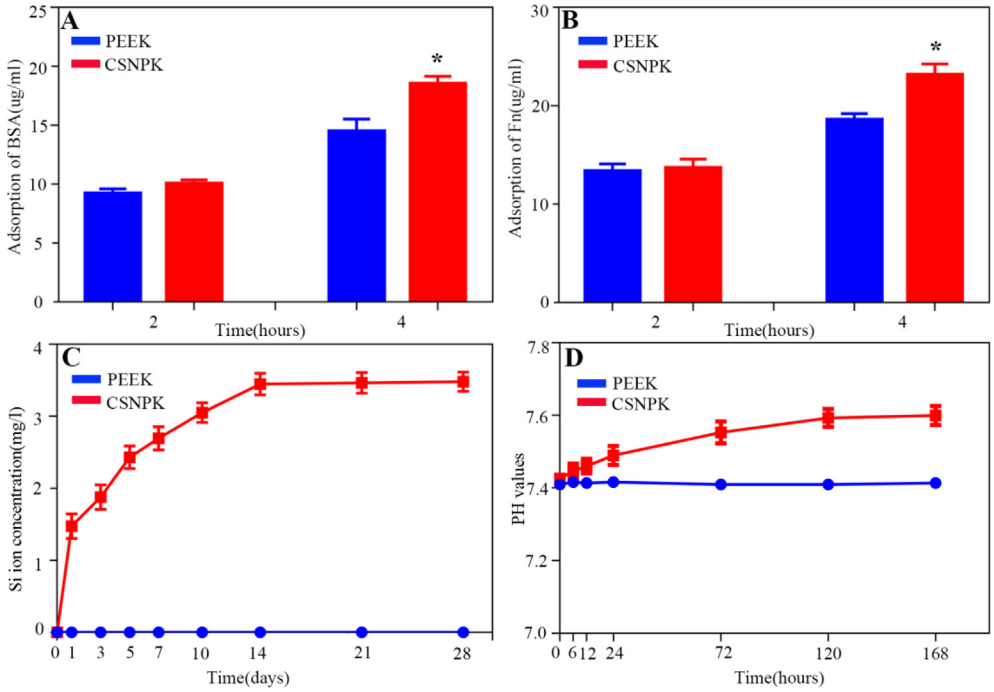


**Figure 3.** (A) Adsorption of BSA on PEEK and CSNPK, (B) Adsorption of Fn on PEEK and CSNPK, (C) Changes of Si ion concentration in solution after PEEK and CSNPK soaking into SBF for different time, (D) Changes of pH values in solution after PEEK and CSNPK soaking into SBF for different time (* represent $p < 0.05$). BSA = bovine serum albumin; Fn = fibronectin; PEEK = polyetheretherketone; SBF = simulated body fluid.

of calcium nodule formation on the samples at 21 and 28 d after culturing. The calcium nodule formation for CSNPK was higher than for PEEK at 21 and 28 days, showing that the differentiation of the cells on CSNPK was more than on PEEK.

*Bone-related genes expressions*

Figure 7 shows the expressions of bone-related genes (ALP, COLI, OPN, OCN) of the cells on the samples at 7, 14, and 21 days after culturing. The results revealed that the expressions of ALP (Figure 7A) and COLI (Figure 7B)

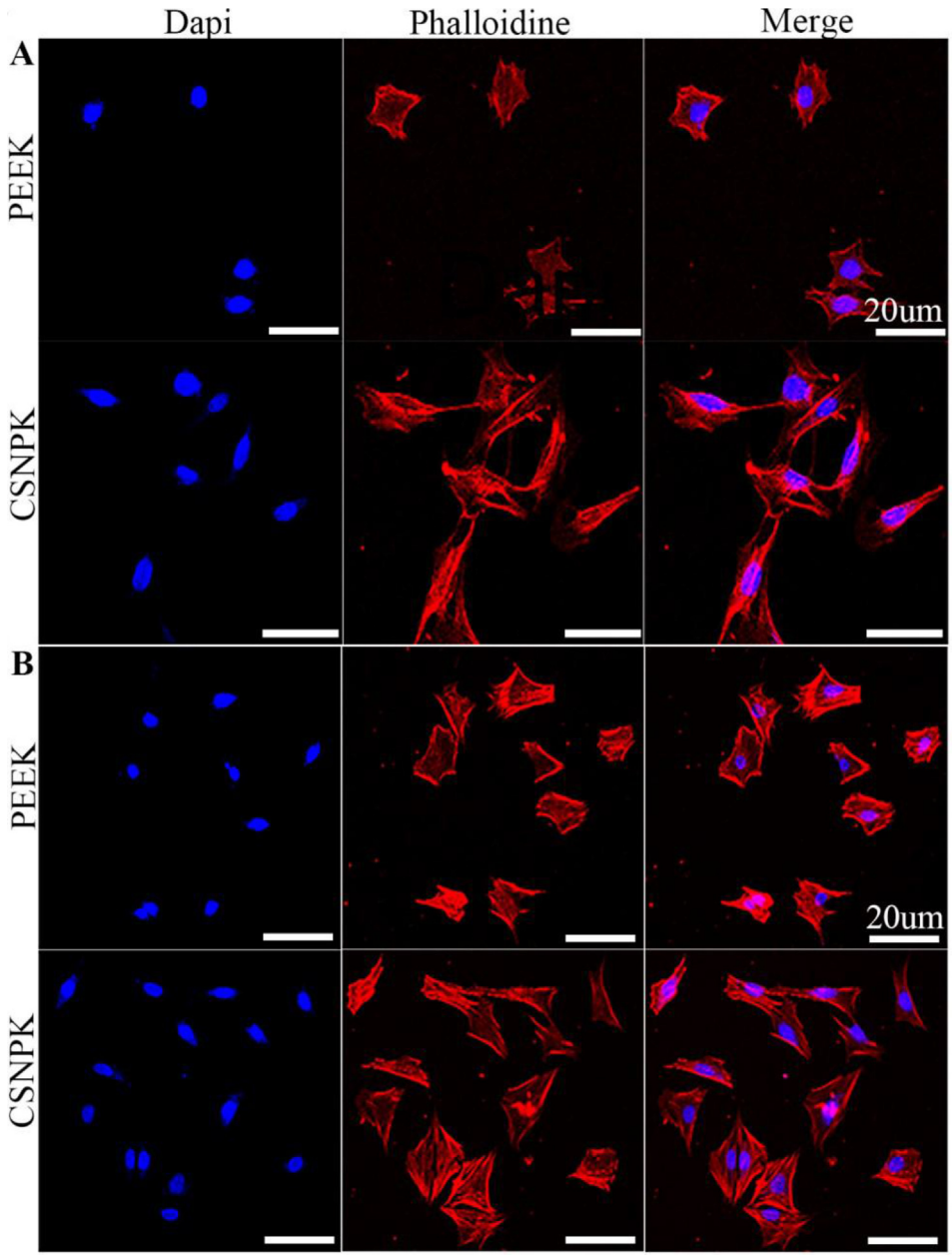


**Figure 4.** (A) CLSM images of MC3T3-E1 cells on PEEK and CSNPK for 12 hours, (B) CLSM images of MC3T3-E1 cells on PEEK and CSNPK for 24 hours by fluorescence staining: Dapi for cell nuclei (blue), phalloidin for actin filaments (red) and merge image (scale bar = 20μm). CLSM = confocal laser scanning microscopy; PEEK = polyetheretherketone.

of the cells for CSNPK were higher than for PEEK at different times ($p < 0.05$). Moreover, the expressions of OPN (Figure 7C) for CSNPK were higher than for PEEK at 14 and 21 days ($p < 0.05$), and the expressions of OCN (Figure 7D) for CSNPK were higher than for PEEK at 21 days ($p < 0.05$).

*Osteogenesis in vivo*

*Micro-CT evaluation*

Figure 8A shows the 3D reconstructed images from micro-CT of the samples. The results revealed that the NBs for CSNPK were higher than for PEEK at both 4 and 8 weeks. Figure 8B and C shows the quantitative analysis of BV/TV (Figure 8B) and BMD (Figure 8C) within the bone defects of skulls of rats at 4 and 8 weeks. The BMD and BV/TV for CSNPK were significantly higher than for PEEK ($P < 0.05$).

*Histological evaluation*

Figure 9A–D shows the histological images of H&E staining after PEEK (Figure 9A and B) and CSNPK (Figure 9C and D) implanted *in vivo* for different times. At 4 weeks, the NBs were hardly observed on PEEK (Figure 9A) while some NBs were found on CSNPK (Figure 9C). At 8 weeks, the NBs were still limited (some fibrous tissues were found) for PEEK (Figure 9B) while more NBs were found on CSNPK (Figure 9D). The results showed the NBs on CSNPK were obviously higher than on PEEK. Furthermore, the NBs were more closely combined with CSNPK.

Figure 9E–H shows the histological images of Masson staining after PEEK (Figure 9E and F) and CSNPK (Figure 9G and H) implanted *in vivo* for different times. At 4 weeks, few NBs were found on PEEK (Figure 9E) while some NBs were found on CSNPK (Figure 9G). At 8 weeks, the NBs were still limited (some fibrous tissues were found) for PEEK (Figure 9F)

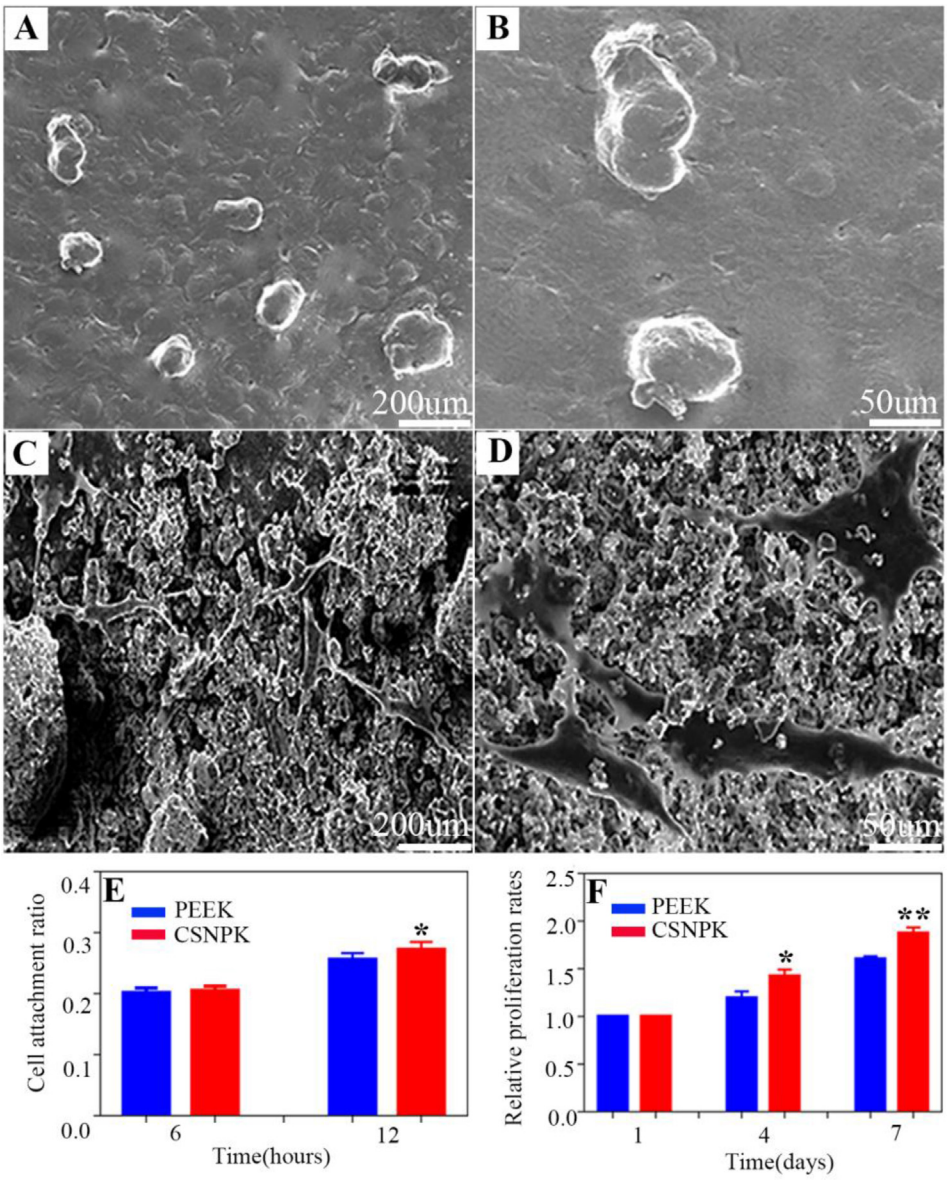


**Figure 5.** (A, B) SEM images of the cells morphology on PEEK at 12 hours under different magnification, (C, D) SEM images of the cells morphology on CSNPK at 12 hours under different magnification, (E) Attachment ratio of the cells on the samples at 6 and 12 hours, (F) Relative proliferation rates of cells on the samples at 1, 4 and 7 d (*$p < 0.05$ compared with PEEK, **$p < 0.05$ compared with PEEK). PEEK = polyetheretherketone; SEM = scanning electron microscope.

while more NBs were found on CSNPK (Figure 9H). The results showed that the NBs on CSNPK were significantly higher than on PEEK. Furthermore, the NBs were more closely combined with CSNPK.

## Discussions

Osseointegration of an implantable material is crucial for not only initial load/fixation but also long-term stability of orthopaedic implants [20]. Hence, the implantable materials should possess excellent biocompatibility and bioactivity (osteoconductivity), which could be integrated with host bone tissues (known as osseointegration) [21]. In this work, to improve the osteoconductivity of PEEK, a bioactive SN coating was created on PEEK surface by the method of suspension coating and melt bonding. The results showed that the coating of CSNPK contained not only SN microparticles but also SN nanoparticles, which caused micronanostructures on CSNPK surface. Moreover, the SN coating with thickness of approximately 10 μm was closely combined with the substrate of PEEK, and the adhesive strength between the coating and substrate was 7.9 MPa. Previous study has shown that the adhesive strength of hydroxyapatite coating on Ti by plasma-spray was 7 MPa [22]. Therefore, the adhesive strength of the SN coating with PEEK was almost similar to the hydroxyapatite coating with Ti [22].

The surface properties (such as roughness and hydrophilicity) have obvious effects on the biological performances of the biomaterials [23]. Increase of surface roughness of biomaterials can promote the cells attachment, proliferation, and differentiation [24]. Moreover, the hydrophilic surface of biomaterials tends to enhance the early stages of adhesion and proliferation of cells compared with hydrophobic surfaces [25]. Previous study has shown that the surface of SN could naturally form hydroxyl (-OH) groups and amino ($-NH_2$) groups in water or biological environment, which improved the hydrophilicity of SN [13]. In this study, the surface roughness of CSNPK with SN coating was significantly higher than PEEK. In addition, the hydrophilicity of CSNPK was obviously higher than that of PEEK. Hence, the improvements in surface roughness and hydrophilicity of CSNPK were ascribed to the SN coating of CSNPK compared with PEEK.

The rapid adsorption of proteins onto the surface of implantable materials is the first step in their exposure to the biological environment,

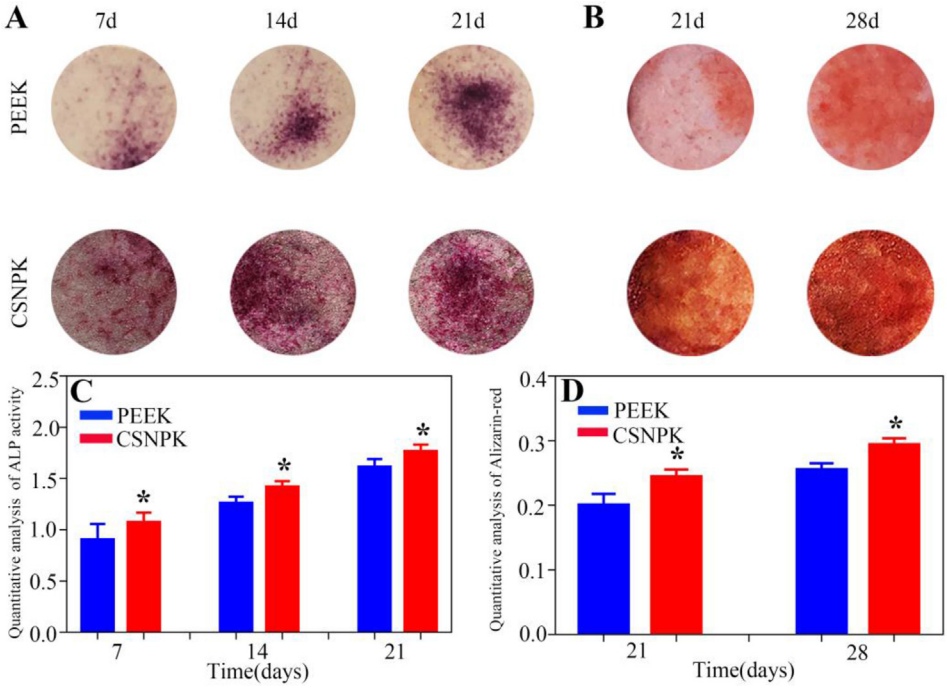


**Figure 6.** (A) ALP staining of the cells on the samples at 7, 14 and 21 days after culturing, (B) ARS staining of the cells on the samples at 21 and 28 days after culturing, (C) Quantitative analysis of ALP activity of the cells on the samples at 7, 14 and 21 days after culturing, (D) Quantitative analysis of Alizarin-red of the cells on the samples at 21 and 28 days after culturing (*$p < 0.05$ compared with PEEK). ALP = alkaline phosphatase; ARS = alizarin red staining; PEEK = polyetheretherketone.

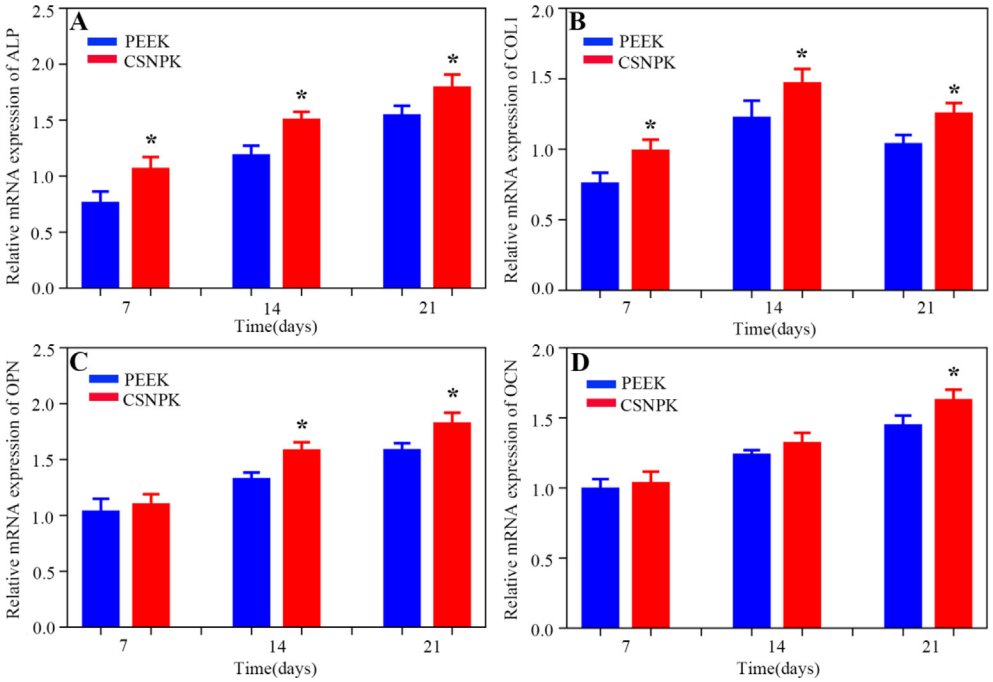


**Figure 7.** (A) Relative mRNA expressions of ALP of cells on the samples at 7, 14 and 21 d after culturing, (B) Relative mRNA expressions of COLI of cells on the samples at 7, 14 and 21 d after culturing, (C) Relative mRNA expressions of OPN of cells on the samples at 7, 14 and 21 d after culturing, (D) Relative mRNA expressions of OCN of cells on the samples at 7, 14 and 21 d after culturing (*$p < 0.05$ compared with PEEK). ALP = alkaline phosphatase; COL1 = collagen type I; OCN = osteocalcin; OPN = osteopontin; PEEK = polyetheretherketone.

which triggers cell activation [25]. Serum albumin, a major transport protein, which plays key roles in regulating the behaviours and functions of osteoblasts [26]. In addition, Fn plays important roles in mediating cell/biomaterial interactions, which provide integrin-binding sites for cell adhesion [27]. Previous study showed that rough and hydrophilic surface could increase the amount of protein adsorption [28]. In this study, the adsorption of both BSA and Fn on CSNPK surface was higher than on PEEK. Accordingly, the increase of protein adsorption of CSNPK was attributed to the SN coating with high surface roughness and hydrophilicity compared with PEEK. Si ions, the dissolution product of bioactive glasses, were found to be effective in regulating the proliferation, differentiation, and expression of osteoblastic markers [29]. In this study, no Si ion released from PEEK while Si ions slowly released from CSNPK into SBF. In addition, there was no change of pH values with time in SBF for PEEK while the pH values for CSNPK slightly increased with time and formed a weak alkaline microenvironment, which is generally

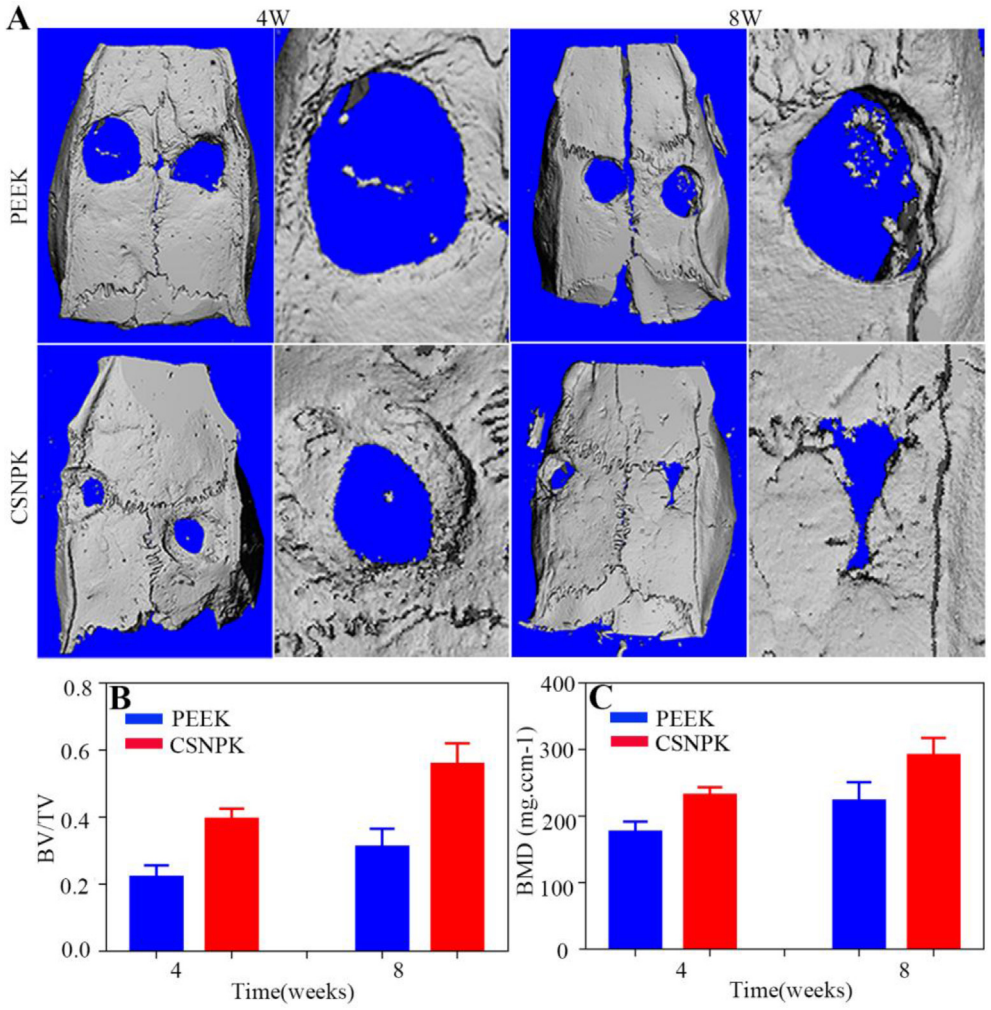


**Figure 8.** (A) Representative 3D reconstructed images from micro-CT after the samples implanted *in vivo* (defects of skulls of rats) for 4 and 8 weeks, (B) Bone volume/tissue volume (BV/TV) within the defects for 4 and 8 weeks, (C) Bone mineral density (BMD) within the defects for 4 and 8 weeks (*$p < 0.05$ compared with PEEK, **$p < 0.05$ compared with PEEK). CT = computed tomography; PEEK = polyetheretherketone.

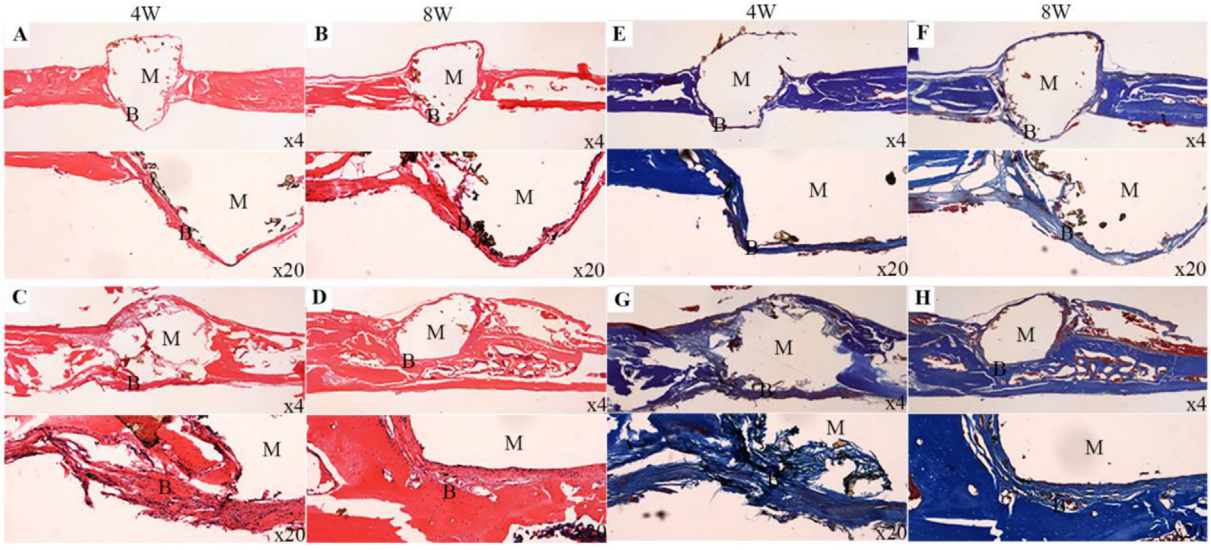


**Figure 9.** (A, B, E, F) Representative histological images (×4, ×20) of H&E and Masson staining after PEEK implanted *in vivo* (longitudinal sections at the defects of skull) for 4 and 8 weeks, (C, D, G, H) Representative histological images (×4, ×20) of H&E and Masson staining after CSNPK implanted *in vivo* (longitudinal sections at the defects of skull) for 4 and 8 weeks (M: materials, B: bone). PEEK = polyetheretherketone.

considered to be suitable for cells growth [30]. Clearly, the release of Si ion from the SN coating of CSNPK and formation of weak alkaline microenvironment were attributed to slight dissolution of SN in SBF.

Cell adhesion is the first step of cell responses to the biomaterials, which further affects cells spreading and proliferation on the surface [31]. Osteoblasts adhere onto the substrates via integrins, which interact with its ligand and trigger signalling that promotes cytoskeletal changes, leading to cell spreading through the process termed "outside-in signaling" [32,33]. The expression of integrins is dependent on surface roughness, microstructure, and hydrophilicity of the biomaterial [34]. In this study, the cells on CSNPK displayed better adhesion and spreading morphology with more pseudopods than on PEEK. Moreover, the cells attachment ratio on CSNPK was obviously higher than on PEEK. Therefore, compared with PEEK, CSNPK obviously promoted cell adhesion and spreading, indicating that bioactive SN coating of CSNPK played vital roles in facilitating cells adhesion and spreading. After cell adhesion and spreading, the proliferation of the cells on the implantable material is the second critical phase of the bone regeneration [35]. In this work, the cells proliferation on CSNPK was obviously higher than PEEK, indicating that SN coating promoted cells proliferation.

Osteoblasts differentiation from non–calcium-depositing to calcium-depositing cells is synthesis of ALP, and the ALP activity of cells is considered to be correlated to critical functions such as differentiation [36]. In this work, the area of ALP staining on CSNPK was obviously higher than on PEEK. In addition, by quantitative analysis, the ALP activity of CSNPK was obviously higher than that of PEEK, indicating that CSNPPK with SN coating promoted cells differentiation. Moreover, the area of Alizarin-red staining for CSNPK was higher than for PEEK, showing that the formation of mineralised nodules on CSNPK was higher than on PEEK. Furthermore, by the quantitative analysis, the mineralised nodules of cells on CSNPK were higher than on PEEK, indicating that CSNPK with SN coating promotes the cells differentiation. Moreover, the expressions of bone-related genes (ALP, COLI, OPN, and OCN) for CSNPK were higher than those for PEEK. Therefore, CSNPK significantly improved the expression of bone-related genes, including early-stage makers of ALP and COLI, and late-stage makers of OPN and OCN.

Based on the positive results of *in vitro* studies, the defects of skull models of rats were established for *in vivo* study. From the 3D reconstructed images of micro-CT and quantitative analysis of BV/TV and BMD, the results revealed that the NBs for CSNPK were obviously higher than PEEK at both 4 and 8 weeks. In addition, more NBs were closely combined with the surface of CSNPK while few NBs (formation of fibrous tissues) were combined with PEEK. Clearly, CSNPK exhibited excellent osseointegration while PEEK showed no osseointegration. The results of histological images of H&E and Masson staining showed that the NBs for CSNPK were obviously higher than PEEK at both 4 and 8 weeks, indicating that CSNPK promoted bone regeneration better than PEEK. Furthermore, the NBs were closely combined with the surface of CSNPK while the fibrous tissues formed on PEEK surface, revealing that CSNPK improved osseointegration better than PEEK. Therefore, the results demonstrated that CSNPK with bioactive SN coating promoted bone regeneration and osseointegration better than PEEK *in vivo*.

The surface characteristics (e.g., chemical composition, topological microstructure, roughness, hydrophilicity, and so on) of implantable biomaterials played vital roles in enhancing osteoblasts responses and ultimately improved bone regeneration and osseointegration [25,31,35]. In this study, compared with PEEK, the osteoblasts responses to CSNPK were significantly improved *in vitro*. In addition, the osseointegration of CSNPK was obviously promoted *in vivo*. Therefore, based on the aforementioned studies, it can be suggested that the enhancements of cells responses *in vitro* and promotion of osseointegration *in vivo* were ascribed to the improvements of surface properties (containing chemical composition, roughness, hydrophilicity, protein absorption, and Si ions release) of CSNPK, which were the results of synergistic effects. In summary, CSNPK exhibited good biocompatibility and bioactivity, which have large potentials for orthopaedic applications.

## Conclusions

In this work, to improve the osteoconductivity of PEEK, bioactive SN coating with micro/nano structures on PEEK surface was created by the method of suspension coating and melt bonding. The results demonstrated that the SN coating leads to higher surface roughness, hydrophilicity, and protein absorption of CSNPK than PEEK. In addition, the SN coating of CSNPK could slowly release Si ion into SBF, which caused weak alkaline of microenvironment owing to the slight dissolution of SN. Moreover, compared with PEEK, the SN coating of CSNPK resulted in the improvements of adhesion, proliferation, differentiation, and gene expressions of mouse embryonic osteoblastic precursor cells *in vitro*. Furthermore, the SN coating of CSNPK obviously promoted bone regeneration and osseointegration *in vivo* compared with PEEK. In summary, CSNPK with SN coating as bone implant might be a promising candidate for orthopaedic implants.

## Declaration of competing interest

The authors declare that they have no financial and personal relationships with other people or organisations that can inappropriately influence their work, and there is no professional or other personal interest of any nature or kind in any product, service, and/or company that could be construed as influencing the position presented in, or the review of, the manuscript entitled.

## Acknowledgements

This research was financially supported by the National Key Research and Development Program of China (2018YFC1200204), National Natural Science Fund of China (U1732119), Shanghai Science and Technology Development Fund (15441902500 and 18DZ2291200), and Opening program of Shanghai Key Laboratory of Orthopaedic Implants (KFKT2018003).

## References

[1] Kurtz SM, Devine JN. PEEK biomaterials in trauma, orthopedic, and spinal implants. Biomaterials 2007;28:4845.
[2] Xu X, Li Y, Wang L, Li Y, Pan J, Fu X, et al. Triple-functional polyetheretherketone surface with enhanced bacteriostasis and anti-inflammatory and osseointegrative properties for implant application. Biomaterials 2019;212:98.
[3] Ma R, Tang T. Current strategies to improve the bioactivity of PEEK. Int J Mol Sci 2014;15:5426.
[4] Poulsson AHC, David E, Stefan Z, Karin C, Christoph S, Yash A, et al. Osseointegration of machined, injection moulded and oxygen plasma modified PEEK implants in a sheep model. Biomaterials 2014;35:3717.
[5] Kersten RF, van Gaalen SM, de Gast A, Oner FC. Polyetheretherketone (PEEK) cages in cervical applications: a systematic review. Spine J 2015;15:1446.
[6] Rui M, Tang S, Tan H, Lin W, Wang Y, Jie W, et al. Preparation, characterization, and in vitro osteoblast functions of a nano-hydroxyapatite/polyetheretherketone biocomposite as orthopedic implant material. Int J Nanomed 2014;3949:2014.
[7] Wu X, Liu X, Wei J, Ma J, Deng F, Wei S. Nano-$TiO_2$/PEEK bioactive composite as a bone substitute material: in vitro and in vivo studies. Int J Nanomed 2012;1215: 2012.
[8] Ma R, Tang S, Tan H, Qian J, Lin W, Wang Y, et al. Preparation, characterization, in vitro bioactivity, and cellular responses to a polyetheretherketone bioactive composite containing nanocalcium silicate for bone repair. ACS Appl Mater Interfaces 2014;6:12214.
[9] Zhang C, Dan C, Tang T, Jia X, Cai Q, Yang X. Nanoporous structured carbon nanofiber–bioactive glass composites for skeletal tissue regeneration. J Mater Chem B 2015;3:5300.
[10] Wang J, Li D, Li T, Ding J, Liu J, Li B, et al. Gelatin tight-coated poly(lactide-co-glycolide) scaffold incorporating rhBMP-2 for bone tissue engineering. Materials 2015;8:1009.
[11] Mazzocchi M, Bellosi A. On the possibility of silicon nitride as a ceramic for structural orthopaedic implants. Part I: processing, microstructure, mechanical properties, cytotoxicity. J Mater Sci Mater Med 2008;19:2881.
[12] Mazzocchi M, Gardini D, Traverso PL, Faga MG, Bellosi A. On the possibility of silicon nitride as a ceramic for structural orthopaedic implants. Part II: chemical stability and wear resistance in body environment. J Mater Sci Mater Med 2008;19: 2889.
[13] Bock RM, Mcentire BJ, B Sonny B, Rahaman MN, Marco B, Giuseppe P. Surface modulation of silicon nitride ceramics for orthopaedic applications. Acta Biomater 2015;26:318.

[14] Badran Z, Struillou X, Hughes FJ, Soueidan A, Hoornaert A, Ide M. Silicon nitride ($Si_3N_4$) implants: the future of dental implantology? J Oral Implantol 2017;43:240.
[15] Arts MP, Wolfs JFC, Corbin TP. Porous silicon nitride spacers versus PEEK cages for anterior cervical discectomy and fusion: clinical and radiological results of a single-blinded randomized controlled trial. Eur Spine J 2017;26:2372.
[16] Pezzotti G, Oba N, Zhu W, Marin E, Rondinella A, Boschetto F, et al. Human osteoblasts grow transitional Si/N apatite in quickly osteointegrated $Si_3N_4$ cervical insert. Acta Biomater 2017;64:411.
[17] Pezzotti G, Marin E, Adachi T, Rondinella A, Boschetto F, Zhu W, et al. Bioactive silicon nitride: a new therapeutic material for osteoarthropathy. Sci Rep 2017;7:44848.
[18] Pezzotti G, Marin E, Adachi T, Lerussi F, Rondinella A, Boschetto F, et al. Incorporating $Si_3N_4$ into PEEK to produce antibacterial, osteocondutive, and radiolucent spinal implants. Macromol Biosci 2018:e1800033.
[19] Chu L, Jiang G, Hu X, James TD, He XP, Li Y, et al. Biodegradable macroporous scaffold with nano-crystal surface microstructure for highly effective osteogenesis and vascularization. J Mater Chem B 2018;6:1658.
[20] Fan X, Peng H, Li H, Yan Y. Reconstruction of calvarial bone defects using poly(amino acid)/hydroxyapatite/calcium sulfate composite. J Biomater Sci Polym Ed 2018;30:107.
[21] Mahjoubi H, Buck E, Manimunda P, Farivar R, Chromik R, Murshed M, et al. Surface phosphonation enhances hydroxyapatite coating adhesion on polyetheretherketone and its osseointegration potential. Acta Biomater 2017;47:149.
[22] Karazisis D, Petronis S, Agheli H, Emanuelsson L, Norlindh B, Johansson A, et al. The influence of controlled surface nanotopography on the early biological events of osseointegration. Acta Biomater 2017;53:559.
[23] Bo Y, Chen Y, Hai L, Song Y, Xi Y, Hai T, et al. Processing and properties of bioactive surface-porous PEKK. ACS Biomater Sci Eng 2016;2:977.
[24] Gittens RA, Olivaresnavarrete R, Schwartz Z, Boyan BD. Implant osseointegration and the role of microroughness and nanostructures: lessons for spine implants. Acta Biomater 2014;10:3363.
[25] Gittens RA, Scheideler L, Rupp F, Hyzy SL, Geisgerstorfer J, Schwartz Z, et al. A review on the wettability of dental implant surfaces II: biological and clinical aspects. Acta Biomater 2014;10:2907.
[26] Ishida K, Yamaguchi M. Role of albumin in osteoblastic cells: enhancement of cell proliferation and suppression of alkaline phosphatase activity. Int J Mol Med 2004;14:1077.
[27] Siebers MC, Brugge PJT, Walboomers XF, Jansen JA. Integrins as linker proteins between osteoblasts and bone replacing materials. A critical review. Biomaterials 2005;26:137.
[28] Li Z, Qiu J, Du LQ, Jia L, Liu H, Ge S. $TiO_2$ nanorod arrays modified Ti substrates promote the adhesion, proliferation and osteogenic differentiation of human periodontal ligament stem cells. Mater Sci Eng C-Mater 2017;76:684.
[29] Sun J, Li W, Liu X, Li J, Li B, Wang G, et al. Influences of ionic dissolution products of dicalcium silicate coating on osteoblastic proliferation, differentiation and gene expression. Acta Biomater 2009;5:1284.
[30] Liu W, Wang T, Yang C, Darvell BW, Wu J, Lin K, et al. Alkaline biodegradable implants for osteoporotic bone defects-importance of microenvironment pH. Osteoporos Int 2016;27:93.
[31] Gyorgyey A, Ungvari K, Kecskemeti G, Kopniczky J, Hopp B, Oszko A, et al. Attachment and proliferation of human osteoblast-like cells (MG-63) on laser-ablated titanium implant material. Mater Sci Eng C-Mater 2013;33:4251.
[32] Hitoshi T, Satoshi N, Naoya T, Atsushi O, Hidekazu N, Yohei M, et al. Lnk regulates integrin alphaIIbbeta3 outside-in signaling in mouse platelets, leading to stabilization of thrombus development in vivo. J Clin Investig 2010;120:179.
[33] Phillips DR, Nannizzialaimo L, Prasad KS. Beta3 tyrosine phosphorylation in alphaIIbbeta3 (platelet membrane GP IIb-IIIa) outside-in integrin signaling. J Thromb Haemost 2001;85:246.
[34] Natalia D, Schuster CF, Bax DV, Farndale RW, Samir H, Best SM, et al. Evaluation of cell binding to collagen and gelatin: a study of the effect of 2D and 3D architecture and surface chemistry. J Mater Sci Mater Med 2016;27:148.
[35] Kerativitayanan P, Carrow JK, Gaharwar AK. Nanomaterials for engineering stem cell responses. Adv Healthc Mater 2015;4:1600.
[36] Zhou XJ, Feng W, Qiu KX, Chen L, Wang WZ, Nie W, et al. BMP-2 derived peptide and dexamethasone incorporated mesoporous silica nanoparticles for enhanced osteogenic differentiation of bone mesenchymal stem cells. ACS Appl Mater Interfaces 2015;7:15777.